Complexation of thermoresponsive dialkoxynaphthalene end-functionalized poly(oligoethylene glycol acrylate)s with $CBPQT^{4+}$ in water

Bahar Yeniad,[a] Kanykei Ryskulova,[a] David Fournier,[b] Joël Lyskawa,[b] Graeme Cooke,[c] Patrice Woisel*[b] and Richard Hoogenboom*[a]

Four different oligoethylene glycol acrylates (OEGA), namely hydroxypropylacrylate (HPA), methoxy diethylene glycol acrylate (mDEGA), methoxy triethylene glycol acrylate (mTEGA) and 2-hydroxyethylacrylate (HEA) were homopolymerized via RAFT polymerization employing a naphthalene functionalized chain transfer agent resulting in thermoresponsive naphthalene-functionalized POEGAs with different hydrophilicities. Supramolecular inclusion complexes of these POEGAs with electron-deficient cyclophane cyclobis(paraquat-p-phenylene) tetrachloride ($CBPQT^{4+}$) in water were studied. The association constants (K_a) were determined to study the effect that polymer hydrophilicity has on the K_a and results indicated that the nature of the polymer did not significantly influence the complexation strength and the association is mostly enthalpy driven. The impact of temperature on the host–guest complexes was also investigated. A continuous partial thermally induced dissociation of complexes was observed upon raising the temperature with a more distinct decrease in complexation around the cloud point temperature (T_{CP}) of the POEGA employed, indicating the importance of the polymer phase transition for tuning the recognition properties of dialkoxynaphthalene end-decorated poly(oligoethylene glycol acrylate)s in water.

Introduction

Supramolecular chemistry deals with highly organized structures held together by non-covalent interactions such as Van der Waals forces, hydrophobic interactions or hydrogen bonding. Supramolecular systems have gained great attention in recent years and have been employed in various fields including catalysis, pharmaceutical and biomedical applications, separation technology, food and flavours.[1–3] In particular, the construction of supramolecular assemblies from host–guest inclusion complexes, in which smaller hydrophobic guest molecules are held within the internal cavity of a host molecule, has received considerable attention. Indeed, thanks to the development of highly-specific, directional and stimuli-responsive host–guest type architectures, nano- and macro-assemblies exploiting such interactions have found numerous applications in many key research domains, including nanotechnology, nanomedicine and materials science.[4–7] Many different large molecules with accessible internal cavities have been studied as hosts, cyclodextrins being the most commonly used one thanks to their water solubility, range of cavity size and well-defined internal cavity. The electron-deficient cyclophane cyclobis(paraquat-p-phenylene) ($CBPQT^{4+}$) has emerged as an attractive host unit as well since it can readily form host–guest-specific colored complexes, with electron-rich guests such as 1,5-dialkoxy naphthalene and tetrathiafulvalene[8] derivatives both in organic[9] and aqueous[10] solutions. $CBPQT^{4+}$-based pseudorotaxanes can be reversibly disassembled using a variety of stimuli such as heat,[11–13] pH,[14] oxidation of guest molecules,[15,16] reduction of cyclophane[17] or competitive guest molecules.[18] More recently, cucurbituryl and pillararene based pseudorotoxanes have also become important building blocks for the creation of functional nano- and macro-molecular systems.[19–21]

Polymers displaying lower critical solution temperature (LCST) behavior are of great interest to many research groups as they allow reversible switching of the polymer solubility by

[a]Supramolecular Chemistry Group, Department of Organic and Macromolecular Chemistry, Ghent University, Krijgslaan 281 S4, B9000 Ghent, Belgium. E-mail: Richard.hoogenboom@ugent.be
[b]Université de Lille, ENSCL, Unité des Matériaux et Transformations, UMR CNRS 8207, Equipe Ingénierie des Systèmes Polymères (ISP), 59655 Villeneuve d'Ascq Cedex, France. E-mail: Patrice.woisel@univ-lille1.fr
[c]WestCHEM, School of Chemistry, University of Glasgow, Glasgow, G12 8QQ, UK
†Electronic supplementary information (ESI) available. See DOI: 10.1039/c6py00303f

small variations in temperature.[22,23] Poly(N-isopropylacrylamide) (PNIPAM) is one of the most widely studied LCST polymers since it exhibits LCST behavior at around 32 °C, which is close to body temperature. Recently, polymers bearing a short oligo(ethylene glycol) (OEG) pendant chain have emerged as alternatives to PNIPAM.[24–27] These polymers can be formed from a variety of monomers comprising an OEG chain and a polymerizable group such as a (meth)acrylate, acrylamide or styrene via controlled radical polymerization techniques, e.g. reversible addition–fragmentation chain transfer (RAFT) polymerization, atom transfer radical polymerization (ATRP) and nitroxide mediated polymerization (NMP).[28–32] The phase transition temperature of these polymers, i.e. the cloud point temperature (T_{CP}), can simply be tailored by choosing a monomer with the right number of OEG units in the side chain or by copolymerizing two monomers. In addition, RAFT polymerization allows the synthesis of tailor-made poly(oligo(ethylene glycol) acrylate)s (POEGAs) with different chain end-functionalities by the use of functional chain transfer agents.

In recent years the tuning of polymer phase transition temperatures by supramolecular interactions has emerged as a novel strategy.[33] The end-functionalization of thermoresponsive polymers with various hydrophobic guest molecules and the interaction of these hydrophobic end-groups with supramolecular hosts has been shown to be an effective way to alter polymer phase transition temperatures.[34–36] For example, β-cyclodextrin has been exploited to tune the LCST of end-functionalized PNIPAMs bearing a pyrenyl group by the selective complexation of hydrophobic chain ends, resulting, due to the masking effect of the hydrophilic host molecule, in an increase of the T_{CP} of polymers.[37] Woisel and co-workers have shown that the LCST phase transition temperature of 1,5-dialkoxynaphthalene-terminated PNIPAM could be increased by ca. 6 °C upon addition of $CBPQT^{4+}$ due to the host–guest interaction of the dialkoxynaphthalene moiety and $CBPQT^{4+}$ in water.[13] Moreover the LCST phase transition of PNIPAM was used as a tool to reversibly control this host–guest interaction. The obtained pseudorotaxane-like PNIPAM–$CBPQT^{4+}$ complex could be easily disassembled above the T_{CP} of PNIPAM and subsequently reassembled by lowering the temperature below its T_{CP} which was accompanied by a clear color change. The same group reported the formation of pseudorotaxane-like supramolecular diblock copolymers employing complementary $CBPQT^{4+}$-terminated PNIPAM and tetrathiafulvalene (TTF) end-functionalized poly(N,N-dimethylacrylamide) (PDMAc) or poly(ethyleneoxide) (PEO) in water. In this case, the $CBPQT^{4+}$/TTF-based host–guest complex remained intact and the diblock architecture was retained upon increasing the temperature above the T_{CP} of PNIPAM. However, the LCST phase transition of PNIPAM triggered the self-assembly to form aggregates consisting of collapsed PNIPAM chains surrounded by PDMAc.[38] Scherman and coworkers have also reported the use of a ternary cucurbit[8]uril/methyl viologen based complex to promote a shift of over 5 °C of the T_{CP} of an end-decorated PNIPAM incorporating a hydrophobic dibenzofuran moiety. Interestingly, subsequent decomplexation upon adding a competitive guest allowed the uncomplexed polymeric material to be released and thus its original T_{CP} to be recovered.[39] Side-chain host–guest interactions were also employed to tune polymer phase transition temperatures of thermoresponsive polymers. For example, Zhu et al. reported a copolymer composed of NIPAAM, N,N-dimethylacrylamide and a methacrylate bearing cholic acid pendant groups, and the variation of its T_{CP} upon the addition of different amounts of βCD, due to the host–guest complexation of pendant cholic acid groups with βCD. This variation could be reversed by the addition of a competitive guest molecule to this copolymer–βCD complex.[40] A similar approach was also exploited by Ritter and coworkers to manipulate the thermoresponsive solution behavior of N-isopropylacrylamide copolymers with adamantyl groups in the side-chains in the presence of 2,6-dimethyl-β-CD.[41] In another study, a thermoresponsive random copoly(2-oxazoline) based on 2-ethyl-2-oxazoline (EtOx) and 2-nonyl-2-oxazoline (NonOx), and the increase in its T_{CP} by the addition of different supramolecular hosts such as β-CD, β-(hydroxylpropyl)cyclodextrin and cucurbit[7]uril, was reported. The extent of this increase was found to be dependent on the concentration of the host molecule added and the strength of the complexation between nonyl side-chains and the host molecule.[42]

It is clear that the combination of supramolecular hosts with thermoresponsive polymers displaying complementary and specific recognition properties represents a straightforward strategy to finely modulate the solution behavior of thermoresponsive polymers.[33] Nonetheless, there are surprisingly few studies focusing on the fundamental aspects of how thermoresponsive polymers can influence host–guest complexation as the majority of reports are proof of concept studies showing that the host–guest interactions can influence the T_{CP}.

In this study, we address the fundamental question whether the polymer phase transition induces host–guest disassembly in thermoresponsive supramolecular polymer host–guest complexes or whether the temperature increase is responsible for the disruption of such host–guest complexes. In order to investigate this question, naphthalene end-functionalized POEGAs with different hydrophilicities and hence displaying different T_{CP}s, were prepared. These homopolymers were used to prepare supramolecular inclusion complexes with $CBPQT^{4+}$,$4Cl^-$ in water and the effect of the hydrophilicity of the polymer backbone on the host–guest interaction of 1,5-dialkoxynaphthalene and $CBPQT^{4+}$,$4Cl^-$ was studied by subjecting these solutions to different temperatures. Furthermore the association constants (K_a) in water were determined and compared to study the influence of polymer hydrophilicity.

Results and discussion

Synthesis of the dialkoxynaphthalene functionalized poly(oligoethylene glycol acrylate)s

To vary the hydrophilicity and T_{CP} of the polymers, four different oligoethylene glycol acrylates, namely hydroxypropyl-

acrylate (HPA 1; a mixture of isomers containing 2-hydroxypropylacrylate and 1-methyl-2-hydroxyethylacrylate in a 3 : 1 ratio),[43] methoxy diethylene glycol acrylate (mDEGA 2), methoxy triethylene glycol acrylate (mTEGA 3) and 2-hydroxyethylacrylate (HEA 4, Fig. 1) were chosen and homopolymerized via RAFT polymerization employing a naphthalene functionalized chain transfer agent (5) resulting in naphthalene-functionalized POEGAs (P1–P4) with different hydrophilicities as depicted in Fig. 1 for mDEGA. Polymerizations were performed in the presence of the RAFT agent 5 at 70 °C with 2 M monomer concentration in N,N-dimethylformamide using AIBN as the initiator. In addition to naphthalene-functionalized POEGAs, a reference POEGA was synthesized by polymerizing mDEGA in the presence of non-functional CTA 7 that is denoted as P(mDEGA)* or P2*. Unlike the other four polymers, P2* does not bear the naphthalene moiety at the chain end and it was used as a control sample in supramolecular host–guest complexation studies, where it should be mentioned that the carboxylic acid end-group will be (partially) ionized in MilliQ water further enhancing its hydrophilicity.

Kinetic plots are depicted in Fig. 2 for all four RAFT polymerizations and reveal linear first order kinetics. It should be noted that an inhibition period was found for some RAFT polymerizations, especially for HPA, which is commonly observed for RAFT mediated polymerizations probably due to different levels of residual oxygen especially when performed on a small scale. Furthermore, an approximate linear increase of M_n with increasing conversion as well as low dispersities (Đ) indicated

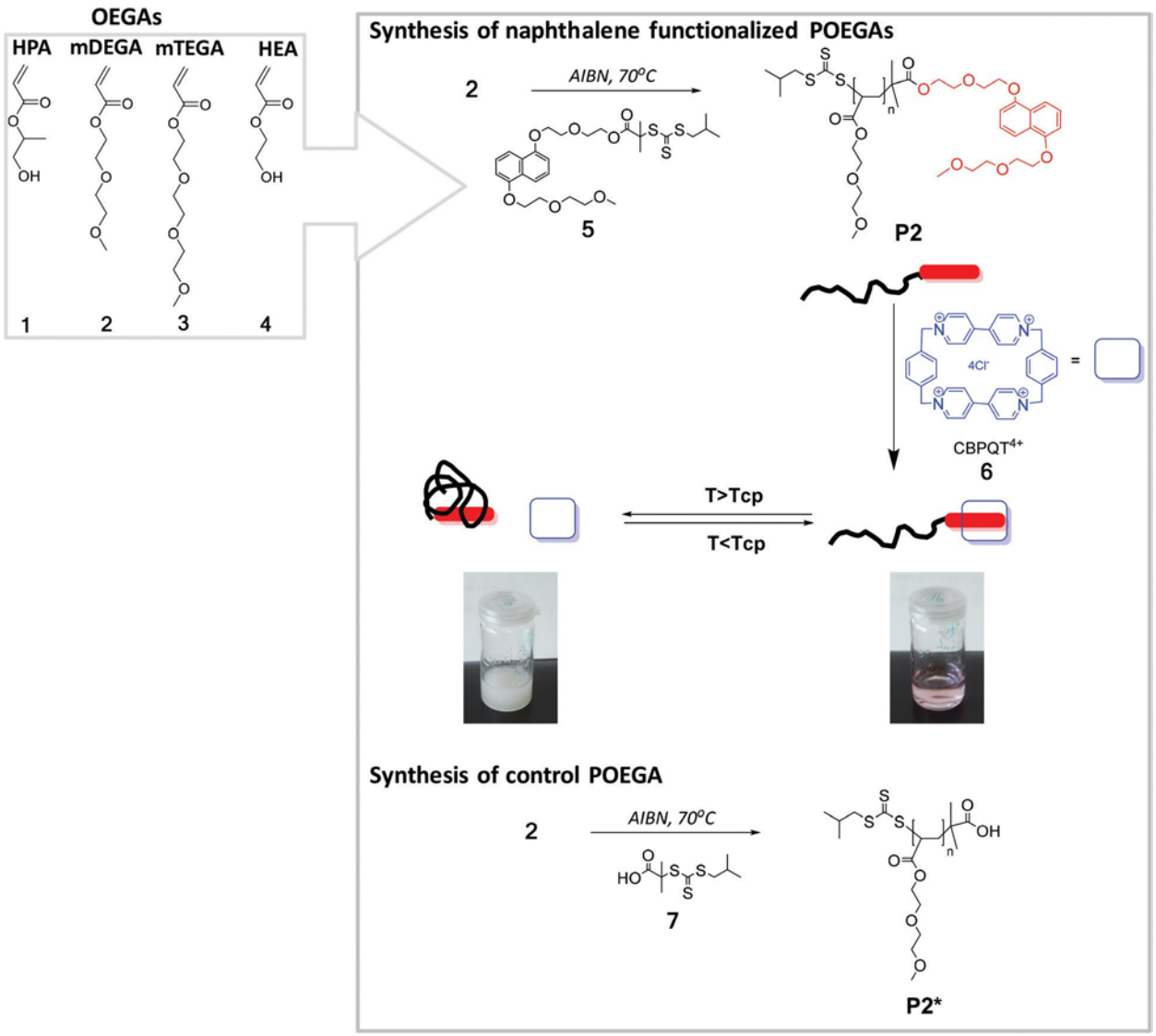

Fig. 1 Left: (Oligo)ethylene glycol acrylates (OEGAs) used in this study. Right: Polymerization and functionalization of OEGAs with the naphthalene moiety via RAFT-polymerization (P2 is shown as a representative example), the effect of temperature on their supramolecular inclusion complexes with $CBPQT^{4+}$,$4Cl^-$ in water, namely collapse of the polymer and disruption of the host–guest complex, and synthesis of the control polymer P(mDEGA)* (P2*).

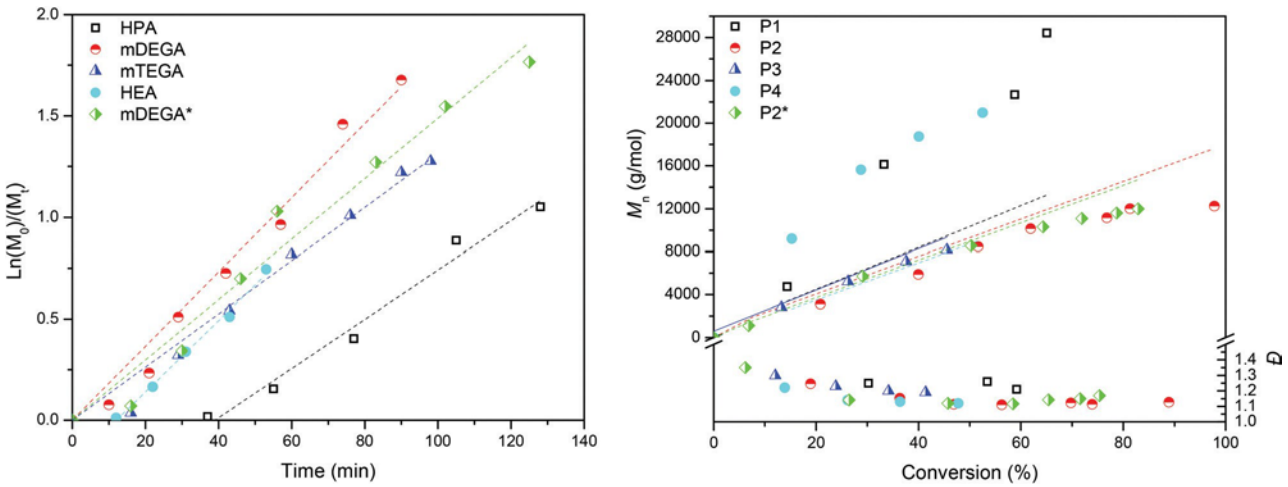

Fig. 2 First order kinetic plot of $\ln([M]_0/[M]_t)$ versus time in the RAFT polymerizations of OEGAs 1–4. The dashed line represents linear fitting of the data after the inhibition period. Right: The number-average molecular weight (M_n) and dispersity (Đ) versus conversion plot. The dashed line represents theoretical number-average molecular weight ($M_{n,th}$; calculated from the monomer to initiator ratio and monomer conversion). (* denotes the control polymer without the naphthalene end-group.)

a controlled radical polymerization of OEGAs with both 5 and 7, where the minor negative deviation from linearity at higher conversions could indicate some chain transfer, although this is not resembled in the Đ values. Size exclusion chromatography traces for samples taken during the homopolymerizations of the OEGAs can be found in Fig. S1.† The characterization data of the obtained naphthalene functionalized POEGAs are summarized in Table 1. The molecular weight of the polymers was calculated by SEC against PMMA standards in DMA. The calculated molecular weights differ significantly due to the difference in their hydrophilic–hydrophobic character and hence in their hydrodynamic volume in DMA. However, the calculation of the degree of polymerization (DP) and number average molecular weights (M_n) of these polymers by NMR (the integrals of the signals of the $(CH_3)_2CH$–CH_2–S of the RAFT end-group and –C(O)O–CH_2–CH_2–O of the monomer at 1.0 and 4.2 ppm, respectively, were used for end group analysis) showed that the molecular weight of all POEGAs was in the same range, which is important to eliminate the effect of molecular weight in host–guest interactions. The DP values obtained by NMR analysis are significantly lower in many cases than the theoretical DP (DP_{th}) based on GC conversion, which may be due to differences in the solubility of the different molar mass fractions in the precipitation solvent mixture indicating a lower solubility of the low molar mass polymer fraction, possibly induced by the naphthalene end-group.

Thermoresponsive properties of the POEGAs

After synthesis of the POEGAs, their T_{CP}s were determined by performing UV-Vis turbidimetry measurements. Aqueous polymer solutions (c = 5 mg mL^{-1}) were successively heated and cooled between 10 and 80 °C and T_{CP}s were determined at 50% transmittance during polymer precipitation in the second heating run (Fig. 3). Turbidimetry measurements on P2 and the corresponding reference polymer P2* showed a minor ~5 °C decrease in the T_{CP} of the polymer when replacing the slightly hydrophobic naphthalene moiety end-group of P(mDEGA) with the more hydrophilic carboxylic acid moiety (Fig. S2†). The addition of an equimolar amount of $CBPQT^{4+}$,$4Cl^-$ to solutions of P1, P2 and P3, in contrast, increased the T_{CP} of the polymers up to 6 °C depending on the nature of the POEGA. This increased hydrophilicity can be attributed to host–guest interactions of the dialkoxynaphthalene unit with $CBPQT^{4+}$,$4Cl^-$ which has a higher hydrophilicity, due to its cationic nature, than the naphthalene group. To verify this interpretation, it was confirmed that the T_{CP} of P2* did not increase upon addition of $CBPQT^{4+}$. Furthermore, P4

Table 1 Characterization data for the purified pOEGAs

Polymer	OEGA	[M] : [CTA] : [I]	M_n (g mol^{-1}) (SEC)	M_n (g mol^{-1}) (NMR)	Đ	DP (NMR)	Conversion (DP_{th}) (GC)
P1	HPA	[100] : [1] : [0.1]	26 700	8900	1.18	64	65 (65)
P2	mDEGA	[125] : [1] : [0.25]	13 000	10 500	1.13	57	68 (85)
P3	mTEGA	[150] : [1] : [0.1]	11 300	10 400	1.19	45	46 (69)
P4	HEA	[150] : [1] : [0.1]	27 000	8000	1.17	64	53 (80)
P2*	mDEGA*	[100] : [1] : [0.1]	9200	11 000	1.19	55	63 (63)

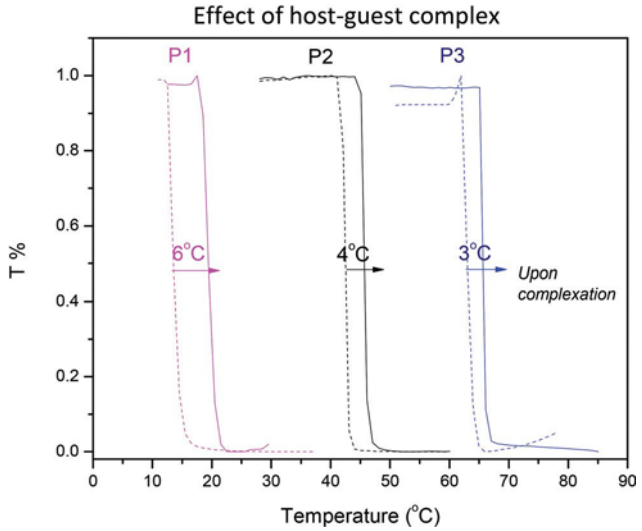

Fig. 3 Left: Thermo-sensitive phase transitions of P1 (pink), P2 (black), P3 (blue), in absence (dotted lines) and presence (solid lines) of $CBPQT^{4+}$,$4Cl^-$ (5 mg mL^{-1} in water). Recorded at 700 nm. Heating rate: 1 °C min^{-1}.

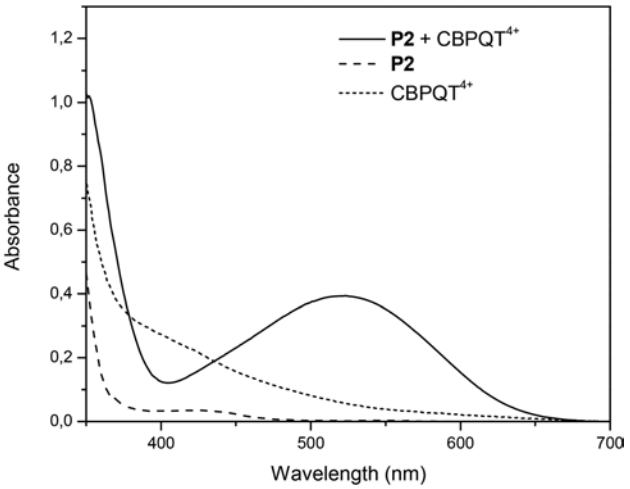

Fig. 4 UV-Vis spectra of P2 (dashed line), $CBPQT^{4+}$,$4Cl^-$ (dotted line) and P2 in the presence of $CBPQT^{4+}$,$4Cl^-$ (solid line) recorded at 10^{-3} M in H_2O at 25 °C.

and its host–guest complex with $CBPQT^{4+}$,$4Cl^-$ are very hydrophilic and did not exhibit a T_{CP} in the studied temperature range, thus being an important polymer to judge whether only increasing the temperature, without the collapse of the polymer, can lead to disruption of the host–guest complexes, vide infra (Fig. S3†).

Host–guest complexation of dialkoxynaphthalene end-functionalized POEGAs with $CBPQT^{4+}$,$4Cl^-$

To further confirm that the increase in T_{CP} upon addition of $CBPQT^{4+}$,$4Cl^-$ indeed results from host–guest complexation, UV-vis spectra were recorded before and after addition of $CBPQT^{4+}$,$4Cl^-$. Upon addition of an equimolar amount of $CBPQT^{4+}$ to 10^{-3} M (with respect to naphthalene functionality) solutions of P2–P4, the formation of the host–guest complexes was clearly visible by the color change of the solutions from colorless to purple, which is characteristic for dialkyloxy-naphthalene–$CBPQT^{4+}$ complexes (Fig. 1). The formation of host–guest complexes was also confirmed by the appearance of an absorption band centered at around 520 nm in the UV-Vis spectrum of the complex. The UV-Vis spectra of P2, $CBPQT^{4+}$,$4Cl^-$ and P2 in the presence of $CBPQT^{4+}$,$4Cl^-$ are shown as a representative example in Fig. 4.

The purple color of the polymer solution was retained in all the complexes upon heating until the temperature exceeded the T_{CP} of the polymers. Once the T_{CP} was exceeded, the hydrophobic collapse of the polymer accompanied by the disappearance of the purple color was observed clearly indicating the disassembly of the host–guest complex. However, this disassembly was reversible and all the complexes could be reassembled by decreasing the temperature below the T_{CP} of the polymers. Importantly, the color of the PHEA solution, which does not have a T_{CP}, remained purple up to 90 °C demonstrating that the hydrophobic collapse of the polymer induces host–guest complex disruption. It can, therefore, be concluded that the polymer phase transition leads to the disruption of the host–guest complexation. This can be rationalized by the fact that the microenvironment of the polymer, and thus also of the host–guest complex, changes from water to the less polar, partially dehydrated polymer chains. Considering that one of the main driving forces for the host–guest complexation in water are hydrophobic interactions this will lead to a less efficient host–guest complexation. Furthermore, the $CBPQT^{4+}$,$4Cl^-$ host molecule is very hydrophilic by nature and will prefer an aqueous environment over the collapsed polymer environment.

UV-Vis and ^1H NMR spectroscopy of host–guest complexes at different temperatures

More in depth analysis was performed by recording the UV-Vis spectra of the obtained complexes (P2, P3 and P4 all with $CBPQT^{4+}$,$4Cl^-$) at different temperatures (Fig. 5). P1 with $CBPQT^{4+}$,$4Cl^-$ was not investigated at high temperatures due to its very low T_{CP}. The intensity of the absorption band at 520 nm, which is characteristic of the host–guest complex of naphthalene and $CBPQT^{4+}$,$4Cl^-$, decreased upon increasing the temperature indicating a drop in K_a leading to partial dissociation of the host–guest complexes, thereby indicating that the host–guest complexation is mostly enthalpy driven. Nonetheless, the presence of absorbance at 520 nm at any temperature below the T_{CP} indicates that the complex still, at least partially, remained. The complete disruption of the complex only occurred when the polymer phase transition was induced by increasing the temperature above the T_{CP}, which could visually be observed by the loss of the purple color. Note that the UV-vis spectra of the polymer complexes with $CBPQT^{4+}$,$4Cl^-$ could not be recorded above T_{CP} due to clouding of the solutions and are not included in the UV-vis spectra overlays in

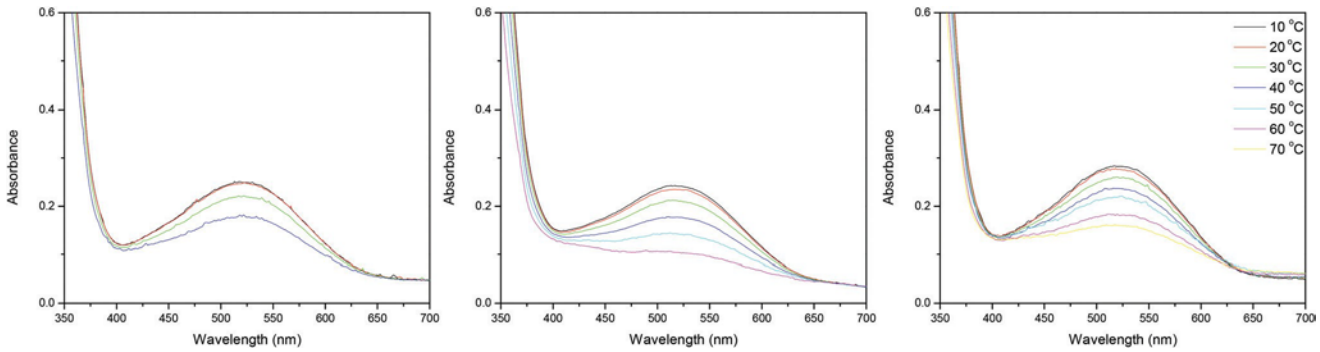

Fig. 5 UV-Vis spectra of host–guest complexes of P2 (left) P3 (middle) and P4 (right) with $CBPQT^{4+},4Cl^{-}$ recorded upon increasing the temperatures (equimolar mixtures at 10^{-3} M).

Fig. 5. Nonetheless, these results suggest that host–guest disassembly was partially induced by elevated temperatures due to a decrease in K_a while the polymer phase transition induced full dissociation. The complete loss of color is, thus, directly related to the polymer phase transition as it also does not occur for PHEA, for which a significant absorption at 520 nm remains in the presence of $CBPQT^{4+},4Cl^{-}$ even at 70 °C.

The effect of temperature on the complexation was also followed by ^{1}H NMR spectroscopy of the polymer–$CBPQT^{4+},4Cl^{-}$ complexes in D_2O at 10^{-3} M (see spectra in Fig. S4–S6†). First of all, it was observed that not all representative signals were clearly visible for both the complexed and free naphthalene for the different polymers indicating a quite different hydration behavior. For P1 with $CBPQT^{4+},4Cl^{-}$ there was a clear signal for the naphthalene incorporated into the host–guest complex around 6.2 ppm at 10 °C, which decreased with increasing temperature, indicative of the loss of the host–guest complex. When heating P1 above the T_{CP} the signal of the naphthalene was no longer observed indicating that it is not well hydrated when the polymer is collapsed.

For P2 and P3 with $CBPQT^{4+},4Cl^{-}$ the complexed naphthalene signal (6.2 ppm) was present at 20 °C while it disappeared from the spectrum at slightly elevated temperatures. This unexpected disappearance of the signal is not fully understood and may be related to a decreased mobility of the naphthalene units and/or a change from the slow exchange to fast exchange of the host–guest complex. When heating towards the polymer T_{CP}, the signals of the free naphthalene appeared around 7.2 ppm, indicative of the loss of the host–guest complex in combination with a relatively high mobility of the naphthalene in the collapsed polymer globules. This higher mobility of the naphthalene groups in the collapsed P2 and P3 compared to the collapsed P1 can be ascribed to the better hydration of these polymers with side-chain oligoethylene glycols in the collapsed state.

After identifying the representative signals, the degree of complexation of P1 with $CBPQT^{4+},4Cl^{-}$ was calculated based on the total integral of the $CBPQT^{4+},4Cl^{-}$ at 9.0–8.7 ppm (calculation with the integrals of the CH_2-group signal of $CBPQT^{4+},4Cl^{-}$ at 5.8 ppm gave the same result) and the complexed naphthalene signal at 6.2 ppm at the different temperatures as plotted in Fig. 6. The maximum degree of complexation observed for P1 at 10 °C to 14 °C is 60–70%, which is in line with the theoretical degree of complexation of 69% at 10^{-3} M with a K_a of ~7000, vide infra. For P2 and P3, the degree of complexation was estimated based on the total integral of the $CBPQT^{4+},4Cl^{-}$ at 9.0–8.7 ppm and the integral of the free naphthalene groups observed around 7.2 ppm.

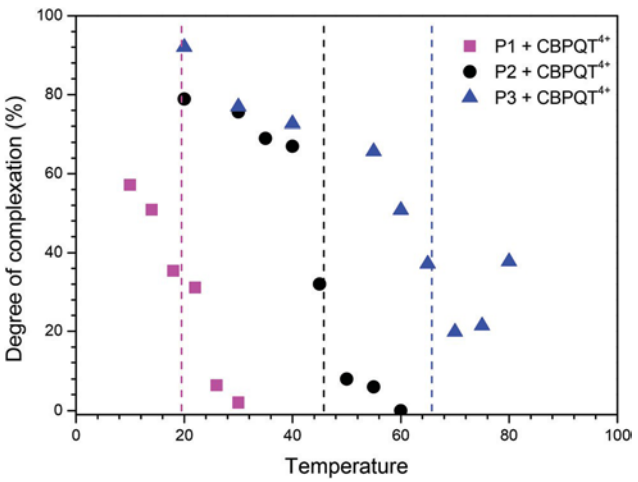

Fig. 6 Percent of complexation of P1, P2 and P3 with $CBPQT^{4+},4Cl^{-}$ as a function of temperature as determined by ^{1}H NMR spectroscopy (equimolar mixtures at 10^{-3} M in D_2O). The dotted lines indicate the cloud point temperatures of the polymers in the presence of $CBPQT^{4+},Cl^{-}$.

A closer look at Fig. 6 reveals that the extent of complexation continuously decreases with increasing temperature, in agreement with the UV-vis results. Moreover, a larger drop in the percent of complexation is seen around the T_{CP} of the polymer after which nearly no complexation is left, confirming that the polymer phase transition induces further disruption of the host–guest complexes. The apparent increase in the degree of complexation for P3 upon heating beyond the T_{CP} is due to the macroscopic precipitation of the polymer leading to a decrease in the naphthalene signal, as also observed for the free polymer by the increase in transmittance after the T_{CP} (Fig. 3) indicating that the collapsed P(mTEGA) is more prone

Table 2 Cloud point temperatures (T_{CP}) of the synthesized POEGAs and calculated K_a values for complexation with $CBPQT^{4+},4Cl^-$ by UV-Vis and ITC

			P1	P2	P3	P4	P2*
T_{CP} (°C)			14	43	66	Soluble	48
K_a ($\times 10^3$ M^{-1})	UV-Vis	12 °C	7 ± 0.8	7 ± 0.8	7.5 ± 0.7	6.7 ± 1.4	
		25 °C	—	3.8 ± 0.3	5.8 ± 0.4	1.0 ± 0.8	
	ITC	12 °C	—	29 ± 3	27 ± 3	55 ± 7	
		20 °C	—	10.5 ± 1.2	13.8 ± 1.5	22.5 ± 0.3	
ΔH (kJ mol^{-1})	ITC	12 °C	—	−56 ± 1	−60 ± 1	−46 ± 1	
		20 °C	—	−47 ± 2	−38 ± 1	−38 ± 1	
ΔS^a (kJ mol^{-1})		12 °C	—	−0.11	−0.13	−0.07	
		20 °C	—	−0.08	−0.05	−0.05	

[a] Calculated from ITC data by using equations $\Delta G = -RT \ln K_a$ and $\Delta S = (\Delta H - \Delta G)/T$.

to macroscopic precipitation as a glue-like substance than the other studied polymers.

Determination of association constants (K_a)

Next, K_a's of the different POEGAs with $CBPQT^{4+},4Cl^-$ were determined by isothermal titration calorimetry (ITC) and UV-Vis titrations to study the effect of polymer hydrophilicity on the K_a. Titrations were performed at 20 °C (ITC) or 25 °C (UV) and 12 °C, the latter temperature was chosen due to the low T_{CP} of P1, i.e. T_{CP} = 14 °C and this polymer was only measured at 12 °C. For ITC titrations, a dilute solution of pOEGA was prepared in deionized water and titrated with a concentrated solution of $CBPQT^{4+},4Cl^-$. The ITC binding isotherms resulting from the addition of $CBPQT^{4+}$ showed sharp exothermic responses. From the ITC curves, K_a's of 10.5 ± 1.2 × 10^3, 13.8 ± 1.5 × 10^3 and 22.5 ± 0.3 × 10^3 were determined for P2, P3 and P4 with $CBPQT^{4+},4Cl^-$, respectively, at 20 °C. These values are an order of magnitude lower than the reported association constant for naphthalene functionalized PNIPAM and $CBPQT^{4+}$.[11] The calculated K_a values correspond to the binding free energies, $\Delta G = -RT \ln K_a$, of −22.9, −23.6 and −24.9 kJ mol^{-1} and binding entropy, $\Delta S = (\Delta H - \Delta G)/T$, of −0.084, −0.051 and −0.045 kJ mol^{-1} for P2, P3 and P4 with $CBPQT^{4+},4Cl^-$, respectively, at 20 °C. The negative ΔH values and insignificant changes in ΔS indicate that the process is enthalpy driven with a value of 38–47 kJ mol^{-1} for each pOEGA. The same experiments were repeated at 12 °C to be able to measure and compare the association constant for P1 with $CBPQT^{4+},4Cl^-$. However, even at 12 °C it was not possible to measure the K_a for P1 with $CBPQT^{4+},4Cl^-$ due to the low T_{CP} of P1. The K_a values calculated at 12 °C for P2, P3 and P4 with $CBPQT^{4+},4Cl^-$ appeared to be slightly higher than those calculated at 20 °C, which confirms that the complexation is mostly enthalpy driven. For UV-Vis titrations, a solution of the naphthalene functionalized polymers with varying amounts of $CBPQT^{4+}$ was prepared. The intensity of the UV-Vis absorption band at 520 nm increased with an increasing concentration of the host molecule and leveled off at a certain concentration of $CBPQT^{4+},4Cl^-$. The K_a values for all polymers were calculated by the non-linear fitting of these titration data and found to be similar for all POEGAs employed (around 7 ± 0.8 × 10^3 M^{-1} at 12 °C). All ITC binding curves and non-linear fitting of UV-Vis titrations can be found in Fig. S7 and S8, respectively, in the ESI.† A summary of the determined K_a values given in Table 2 clearly demonstrates that the nature of the polymer does not significantly affect K_a.

Conclusions

In this study, four well-defined naphthalene end-functionalized POEGAs were prepared via RAFT-mediated polymerization. These thermoresponsive homopolymers displaying different T_{CP}s were used to prepare supramolecular inclusion complexes with $CBPQT^{4+}$ in water. The insertion of the hydrophobic naphthalene moiety as end-group decreased the solvation of the polymer and hence resulted in a decrease in the T_{CP} of the polymer. In contrast, the T_{CP} of the polymers increased up to 6 °C depending on the nature of the POEGA upon complexation with $CBPQT^{4+}$. This increased hydrophilicity was attributed to host–guest interactions of the dialkoxynaphthalene unit with $CBPQT^{4+}$ which has a higher hydrophilicity than the naphthalene group.

The effect of hydrophilicity of the polymer backbone on the host–guest interaction of the 1,5-dialkoxynaphthalene moiety at the polymer chain end and $CBPQT^{4+}$ was studied by recording the UV-Vis spectra of the obtained complexes at different temperatures. The intensity of the characteristic absorption band of the host–guest complex of naphthalene and $CBPQT^{4+}$ was found to decrease upon increasing the temperature, which indicated partial dissociation and loss of the host–guest complexes. However, this absorption band was visible at any temperature below the T_{CP} of the polymer suggesting that the complex was present. The complete disappearance of the color of the host–guest complexes only occurred when the temperature was increased above T_{CP}, indicating that complete decomplexation only occurred when the polymer phase transition of POEGA from a hydrophilic state to a collapsed hydrophobic state was induced. Furthermore, K_a calculations showed that polymer hydrophilicity did not have a big impact on the strength of supramolecular inclusion complexes with $CBPQT^{4+}$ in water.

Experimental section

Materials and instrumentation

2-Hydroxyethylacrylate (HEA) and hydroxypropylacrylate (HPA; a mixture of isomers containing 2-hydroxypropylacrylate and 1-methyl-2-hydroxyethylacrylate in a 3 : 1 ratio)[43] were obtained from Sigma-Aldrich, and N,N-dimethylformamide (DMF) was obtained from Biosolve. Methoxy diethylene glycol acrylate (mDEGA), methoxy triethylene glycol acrylate (mTEGA), cyclophane cyclobis(paraquat-p-phenylene) tetrachloride ($CBPQT^{4+}$), RAFT agents, 5 and 7, were synthesized as described previously.[44,45] All OEGAs were passed through a basic aluminum oxide column before use to remove the inhibitor. 2,2′-Azobis(isobutyronitrile) (AIBN) was obtained from Aldrich and purified by recrystallization in methanol twice. All measurements were performed in MilliQ water.

^{1}H NMR spectra were recorded on a Bruker 300 MHz FT-NMR spectrometer using $CDCl_3$ or acetone-d_6 as the solvent. Chemical shifts (δ) are given in ppm relative to TMS.

Size-exclusion chromatography (SEC) was performed on an Agilent 1260-series HPLC system equipped with a 1260 online degasser, a 1260 ISO-pump, a 1260 automatic liquid sampler, a thermostatted column compartment, a 1260 diode array detector (DAD) and a 1260 refractive index detector (RID). Analyses were performed on two mixed-D columns and a pre-column in series at 50 °C. DMA containing 50 mM of LiCl was used as an eluent at a flow rate of 0.593 ml min^{-1}. The SEC traces were analysed using the Agilent Chemstation software with the GPC add on. The molar mass and Đ values were calculated against PMMA standards.

Gas chromatography was performed on 7890A from Agilent Technologies with an Agilent J&W Advanced Capillary GC column (30 m, 0.320 mm, and 0.25 μm). Injections were performed with an Agilent Technologies 7693 autosampler. Detection was done with a FID detector. Injector and detector temperatures were kept constant at 250 and 280 °C, respectively. The column was initially set at 50 °C, followed by two heating stages: from 50 °C to 100 °C with a rate of 20 °C min^{-1} and from 100 °C to 300 °C with a rate of 40 °C min^{-1}, and then held at this temperature for 0.5 minutes. Conversion was determined based on the integration of monomer peaks using DMA as the internal standard.

Turbidity measurements were performed on a Cary 300 Bio UV-visible spectrophotometer with Peltier temperature control at a wavelength of 700 nm. The samples were first cooled to a suitable temperature to fully dissolve the polymer (5 mg ml^{-1}) in deionized water, after which the sample was placed in the instrument and cooled to 5 °C. In the case of supramolecular host–guest complexes, 1 equivalent of $CBPQT^{4+}$ was added to the polymer solution. The transmittance was measured during at least two controlled cooling/heating cycles with a cooling/heating rate of 1 K min^{-1} from 5 °C to 80 °C with hold steps of 5 min at the extreme temperatures while stirring. The T_{CP} is given as the temperature when the transmittance goes through 50% during the second heating ramp.

UV-vis spectra were recorded on a Cary 300 Bio UV-visible spectrophotometer with Peltier temperature control. The temperature dependent UV-vis spectra shown in Fig. 5 were recorded with a 10^{-3} M polymer concentration and 1 equivalent of $CBPQT^{4+}$ at different temperatures. The determination of the K_a was performed at two different temperatures, 25 °C and 12 °C, at 10^{-3} M polymer concentration and by adding aliquots of $CBPQT^{4+}$ into the guest solution followed by recording the UV-vis spectrum. K_a values were calculated by non-linear fitting performed using the following equation: $dA_{obs} = dA_{complex}K_a[BB]t/(1 + K_a[BB]t)$.

Isothermal titration calorimetry (ITC) experiments were performed using a nano-ITC titration calorimeter from TA Instruments with a standard sample cell volume of 1 mL, at two different temperatures, 20 °C and 12 °C. A 250 μL injection syringe was used with stirring at 400 rpm. pOEGA was dissolved in deionized water and the solutions were degassed gently under vacuum before use. Each titration comprised 25 × 10 μL injections of $CBPQT^{4+}$ (8 mM) into the guest solution ([pOEGA] = 0.8 mM). Control experiments with identical injections of $CBPQT^{4+}$ into deionized water alone were used to correct titration data. ITC data collected during the analysis (black diamonds) were fitted to an independent site model (red line) where one independent site binds one ligand.[46] The fit and the determination of thermodynamic parameters (K_a, n, DH) were achieved by using the TA Instrument ITC analysis software (NanoAnalyze).

Polymerizations. Synthesis of P(mDEGA) as a representative example

A solution of mDEGA (2.5 g, 14.3 mmol), AIBN (4.7 mg, 29 × 10^{-3} mmol) and naphthalene functionalized CTA (67.1 mg, 0.11 mmol) in DMF (5 mL) was deoxygenated by three freeze–thaw cycles. The reaction flask was placed in an oil bath that was preheated to 70 °C. The polymerisation was allowed to proceed for a certain time under an argon atmosphere until the target monomer conversion was achieved as followed by GC. At the end of the polymerisation, the solution was immediately cooled down by inserting the reaction flask into liquid nitrogen. The polymer was isolated by precipitation twice in a cold hexane/diethyl ether mixture. For kinetic studies, samples were withdrawn at regular time intervals and monomer conversion was determined by GC and the molar mass and Đ by SEC.

P(mDEGA): ^{1}H NMR ($CDCl_3$): δ 1.0 (d, $(CH_3)_2CH–CH_2–S$, CTA), 1.4–2.0 (b, $–CH_2–CH$ backbone), 2.2–2.4 (b, $–CH_2–CH$ backbone), 3.1 (d, 2H, $(CH_3)_2CH–CH_2–S$, CTA), 3.4 (s, OCH_3), 3.4–3.7 (b, $–C(O)O–CH_2–CH_2–O–CH_2–CH_2–OCH_3$), 4.2 (b, $–C(O)O–CH_2–CH_2–O$), 6.8 (d, ArH, CTA), 7.3 (t, ArH, CTA) and 7.8 (d, ArH, CTA) ppm.

P(mTEGA): ^{1}H NMR ($CDCl_3$): δ 1.0 (d, $(CH_3)_2CH–CH_2–S$, CTA), 1.3–2.0 (b, $–CH_2–CH$ backbone), 2.2–2.5 (b, $–CH_2–CH$ backbone), 3.1 (d, 2H, $(CH_3)_2CH–CH_2–S$, CTA), 3.4 (s, OCH_3), 3.4–3.8 (b, $–C(O)O–CH_2–CH_2–O–CH_2–CH_2–OCH_3$), 4.2 (b, $–C(O)O–CH_2–CH_2–O$), 6.8 (d, ArH, CTA), 7.3 (t, ArH, CTA) and 7.8 (d, ArH, CTA) ppm.

P(HEA): ^{1}H NMR (acetone-d_6): δ 1.0 (d, $(CH_3)_2CH–CH_2–S–$, CTA), 1.4–2.2 (b, $–CH_2–CH$ backbone), 2.3–2.7 (b, $–CH_2–CH$ backbone), 3.7 (b, $–C(O)O–CH_2–CH_2–OH$), 4.2 (b, $–C(O)O–CH_2–CH_2–OH$), 7.0 (d, ArH, CTA), 7.4 (t, ArH, CTA) and 7.7 (d, ArH, CTA) ppm.

PHPA: ^{1}H NMR ($CDCl_3$): δ 0.5–2.7 (b, $–CH_2–CH$ backbone and $CH–CH_3$), 3.1–4.3 (b, $O–CH_2$ and CHO), 4.9 (b, –CHO), 6.7 (d, ArH, CTA), 7.3 (t, ArH, CTA) and 7.8 (d, ArH, CTA) ppm.

P(mDEGA)*: ^{1}H NMR ($CDCl_3$): δ 0.8 (t, $CH_2–CH_3$, CTA), 1.2–2.0 (b, $–CH_2–CH$ backbone), 2.3 (b, $–CH_2–CH$ backbone), 3.3 (s, OCH_3), 3.4–3.7 (b, $–C(O)O–CH_2–CH_2–O–CH_2–CH_2–OCH_3$), 4.1 (b, $–C(O)O–CH_2–CH_2–O$), 4.8 (b, $CH–CH_3$, CTA) ppm.

Acknowledgements

BY, KR and RH greatly acknowledge Ghent University, FWO-Flanders and BELSPO (IAP VII/5 Functional Supramolecular Systems FS2) for financial support. PW gratefully acknowledges the financial support from the Agence Nationale de la Recherche for funding (STRAPA project, ANR-12-BS08-0005). Tim Courtin and José Martins (Ghent University) are thanked for support with the variable temperature NMR experiments.

References

1 G. Crini, Chem. Rev., 2014, 114, 10940.
2 E. M. M. Del Valle, Process Biochem., 2004, 39, 1033.
3 G. Tiwari, R. Tiwari and A. K. Rai, J. Pharm. BioAllied Sci., 2010, 2, 72.
4 S. Varghese, J. A. A. W. Elemans, A. E. Rowan and R. J. M. Nolte, Chem. Sci., 2015, 6, 6050.
5 B. V. K. J. Schmidt, M. Hetzer, H. Ritter and C. Barner-Kowollik, Prog. Polym. Sci., 2014, 39, 235.
6 M. Freitag and E. Galoppini, Energy Environ. Sci., 2011, 4, 2482.
7 J. Zhang, R. J. Coulston, S. T. Jones, J. Geng, O. A. Scherman and C. Abell, Science, 2012, 335, 690.
8 P. L. Anelli, P. R. Ashton, R. Ballardini, V. Balzani, M. Delgado, M. T. Gandolfi, T. T. Goodnow, A. E. Kaifer and D. Philp, J. Am. Chem. Soc., 1992, 114, 193.
9 D. Philp, A. M. Z. Slawin, N. Spencer, J. F. Stoddart and D. J. Williams, J. Chem. Soc., Chem. Commun., 1991, 22, 1584.
10 M. Bria, G. Cooke, A. Cooper, J. F. Garety, S. G. Hewage, M. Nutley, G. Rabani and P. Woisel, Tetrahedron Lett., 2007, 48, 301.
11 G. Cooke, J. F. Garety, S. G. Hewage, B. J. Jordan, G. Rabani, V. M. Rotello and P. Woisel, Org. Lett., 2007, 9, 481.
12 J. Bigot, D. Fournier, J. Lyskawa, T. Marmin, F. Cazaux, G. Cooke and P. Woisel, Polym. Chem., 2010, 1, 1024.
13 J. Bigot, M. Bria, S. T. Caldwell, F. Cazaux, A. Cooper, B. Charleux, G. Cooke, B. Fitzpatrick, D. Fournier, J. Lyskawa, M. Nutley, F. Stoffelbach and P. Woisel, Chem. Commun., 2009, 5266.
14 C.-H. Sue, S. Basu, A. C. Fahrenbach, A. K. Shveyd, S. K. Dey, Y. Y. Botros and J. F. Stoddart, Chem. Sci., 2010, 1, 119.
15 L. Sambe, F. Stoffelbach, J. Lyskawa, F. Delattre, D. Fournier, L. Bouteiller, B. Charleux, G. Cooke and P. Woisel, Macromolecules, 2011, 44, 6532.
16 J. Bigot, B. Charleux, G. Cooke, F. Delattre, D. Fournier, J. Lyskawa, F. Stoffelbach and P. Woisel, Macromolecules, 2010, 43, 82.
17 A. C. Fahrenbach, Z. Zhu, D. Cao, W.-G. Liu, H. Li, S. K. Dey, S. Basu, A. Trabolsi, Y. Y. Botros, W. A. Goddard and J. F. Stoddart, J. Am. Chem. Soc., 2012, 134, 16275.
18 M. Bria, J. Bigot, G. Cooke, J. Lyskawa, G. Rabani, V. M. Rotello and P. Woisel, Tetrahedron, 2009, 65, 400.
19 K. I. Assaf and W. M. Nau, Chem. Soc. Rev., 2015, 44, 394.
20 S. Gürbüz, M. Idris and D. Tuncel, Org. Biomol. Chem., 2015, 13, 330.
21 H. Zhang and Y. Zhao, Chem. – Eur. J., 2013, 19, 16862.
22 D. Schmaljohann, Adv. Drug Delivery Rev., 2006, 58, 1655.
23 E. S. Gil and S. M. Hudson, Prog. Polym. Sci., 2004, 29, 1173.
24 J.-F. Lutz, O. Akdemir and A. Hoth, J. Am. Chem. Soc., 2006, 128, 13046.
25 J.-F. Lutz, J. Polym. Sci., Part A: Polym. Chem., 2008, 46, 3459.
26 C. Weber, R. Hoogenboom and U. S. Schubert, Prog. Polym. Sci., 2012, 37, 686.
27 G. Vancoille, D. Frank and R. Hoogenboom, Prog. Polym. Sci., 2014, 39, 1074.
28 F. Hua, X. Jiang, D. Li and B. Zhao, J. Polym. Sci., Part A: Polym. Chem., 2006, 44, 2454.
29 K. Skrabania, J. Kristen, A. Laschewsky, O. Akdemir, A. Hoth and J.-F. Lutz, Langmuir, 2007, 23, 84.
30 A. Miasnikova and A. Laschewsky, Polym. Sci., Part A: Polym. Chem., 2012, 50, 3313.
31 P. Dimitrov, N. Toncheva, P. Weda, S. Rangelov, B. Trzebicka, A. Dworak and C. B. Tsvetanov, Macromol. Symp., 2009, 278, 89.
32 C. Boyer, M. R. Whittaker, M. Luzon and T. P. Davis, Macromolecules, 2009, 42, 6917.
33 V. R. de la Rosa, P. Woisel and R. Hoogenboom, Mater. Today, 2016, 16, 44.
34 B. V. K. J. Schmidt, M. Hetzer, H. Ritter and C. Barner-Kowollik, Macromol. Rapid Commun., 2013, 34, 1306.
35 G. Maatz, A. Maciollek and H. Ritter, Beilstein J. Org. Chem., 2012, 8, 1929.
36 H. Ritter, J. Cheng and M. Tabataba, Beilstein J. Org. Chem., 2012, 8, 1528.

37 Q. Duan, Y. Miura, A. Narumi, X. Shen, S.-I. Sato, T. Satoh and T. Kakuchi, J. Polym. Sci., Part A: Polym. Chem., 2006, 44, 1117.
38 L. Sambe, F. Stoffelbach, K. Poltorak, J. Lyskawa, A. Malfait, M. Bria, G. Cooke and P. Woisel, Macromol. Rapid Commun., 2014, 35, 498.
39 U. Rauwald, J. del Barrio, X. Jun Loh and O. A. Scherman, Chem. Commun., 2011, 47, 6000.
40 Y.-G. Jia and X. X. Zhu, Langmuir, 2014, 30, 11770.
41 H. Ritter, O. Sadowski and E. Tepper, Angew. Chem., Int. Ed., 2003, 42, 3171.
42 V. R. de la Rosa, W. M. Naub and R. Hoogenboom, Org. Biomol. Chem., 2015, 13, 3048.
43 R. Hoogenboom, D. Popescu, W. Steinhauer, H. Keul and M. Moeller, Macromol. Rapid Commun., 2009, 30, 2042–2048.
44 X. P. Qiu, F. Tanaka and F. M. Winnik, Macromolecules, 2007, 40, 7069.
45 J.-H. Ryu, R. Roy, J. Ventura and S. Thayumanavan, Langmuir, 2010, 26, 7086.
46 E. Freire, O. L. Mayorga and M. Straume, Anal. Chem., 1990, 62, 950.